

Lukács Lóránd
lukacsl@iit.bme.hu

AUGMENTED REALITY FOR AIRCRAFT CONTROL

Abstract

The paper presents a low computational cost system engineering solution which can be used for the control and navigation of airplanes in low visibility when Instrumental Flight Rules apply. The application presented in the paper uses the orientation and navigation information of a glider aircraft superimposed on images acquired with a wide angle lens camera during flight. Using this method of displaying data, the crucial information needed for aircraft control such as orientation, heading, airspeed, vertical speed, altitude, angle of attack and slip angle of the aircraft can be viewed by pilots without requiring them to lose sight of their visual viewpoints. The paper emphasizes on determining the correct position of the main visual elements on the image plane required for maintaining the desired heading and attitude of the aircraft. The developed method can also be applied for UAVs controlled via video link.

A tanulmány légi járművek irányításához szükséges alacsony számítási költségekkel járó megoldást mutat be, ami alkalmazható rossz látási körülmények közötti vezérlésénél vagy olyan esetekben, amikor műszerrepülési helyzetek lépnek fel. A bemutatott alkalmazás egy vitorlázó repülőgép példáján becsült orientációs és navigációs adatokat helyez széles látószögű videó kamera által rögzített képekre repülés közben. Ez az adatmegjelenítési módszer a repülőgép vezérléséhez szükséges elengedhetetlen információkat, mint orientáció, útirány, repülési sebesség, vertikális sebesség, magasság, állásszög és oldalcsúszási szög értékeket jelenít meg anélkül, hogy a pilóta kényszerítve legyen, hogy szem elől tévéssze a repüléshez szükséges vizuális referenciáit. A cikk fő hangsúlya a repülőgép orientációjához szükséges főbb vizuális elemek képsíkon való helyének meghatározására esik. A módszer videó kapcsolaton keresztül vezérelt embernélküli légi járművek irányításánál is alkalmazható.

Keywords: *heads up display, artificial horizon, aircraft control, UAV control ~ homloküveg kijelző, mesterséges horizon, repülés irányítás, UAV irányítás*

INTRODUCTION

In case of a conventional aircraft or Unmanned Aerial Vehicle (UAV) controlled via video link, by implementing a heads-up display for aircraft control, the critical information required to fly the aircraft is presented in the pilot's forward field of view, which eliminates the need of continual transition from head-down instruments to head-up, out-the window view during critical phases of flight. With the eyes of the pilot focused out in front of the aircraft and viewing the presentation of airspeed, altitude, aircraft heading and attitude, flight path, flight path angle, pilots can achieve greater precision and situational awareness at all times.

The paper presents a head-up display design method on the example of a glider aircraft with an added video camera, GPS and IMU sensory information. Some details of state estimation [9], [10] and image processing [7] used in the paper can be found in earlier publications.

Since the method uses a wide angle lens camera, this approach can be best implemented on unmanned aerial vehicles or UAVs. The main scope of the paper is the determination of correct artificial horizon and velocity vector placement on the image plane when a wide angle lens camera is used as the means for flying the aircraft by instrumental flight rules (IFR).

Commercial fixed mounted head-up displays typically project the visual data on an angled flat transparent surface (also called a combiner) located directly in front of the pilot. Acting as a beam splitter, this redirects the projected image from the projector in a way that allows the pilot to see the field of view and the projected image at infinity at the same time. Combiners may have special coatings that reflect the monochromatic light used to project the necessary imagery and symbology to be displayed while allowing all other wavelengths of light to pass through. The employment of a head-up display system has the proven result of allowing higher piloting precision while having a standardized HUD system enables easier transition between different types of aircraft.

Early head up displays had been employed on military aircraft and were focused on computed gunnery solutions, using aircraft information such as airspeed and angle of attack, thus greatly increasing the accuracy pilots could achieve in air to air battles. Today, we also see HUD's being increasingly available on commercial passenger aircrafts.

Despite showing substantial flexibility in the use of head-up displays on commercial aircraft, basic HUDs displays use the following symbols:

- airspeed, altitude, vertical velocity
- a horizon line (artificial horizon)
- aircraft attitude indicator in the form of a so called 'ladder', displaying the aircraft's pitch and roll relative to the ground's level/horizon in degrees
- turn/bank and slip/skid indicators
- waterline symbol or aircraft boresight- shows where the nose of the aircraft is actually pointing
- course and/or heading – where heading is defined by the angle between the direction in which the vehicle's nose is pointing and a reference direction (e.g. true north)
- Flight Path Vector (Velocity Vector Symbol) - shows where the aircraft is actually going, which is useful for example, in a situation where the aircraft is pitched up but is losing energy. Here, the waterline and velocity vectors do not overlap as the former is above, while the latter is below the horizon line. This information is particularly useful on landing approach, where the pilot can visualize the location on the runway where the aircraft will touch down. The velocity vector symbol also shows if the aircraft is slipping/skidding, a situation that reduces aerodynamic efficiency. Keeping the velocity vector symbol on the waterline symbol allows the pilot to perform level turns at various angles of bank.

Unmanned aerial vehicles lack a pilot in the cockpit and are controlled using a specialized data link with live video feed. The video system of the aircraft consists of one or more video cameras for aircraft control. The limitations of using video cameras for manual aircraft control consist mainly in the narrow field of view of the employed camera system which limits the UAV operator’s situational awareness. This problem can be addressed to a certain degree by using a wide angle lens camera to increase the pilot’s field of view.

The two problems to be overcome when using wide angle lens cameras are the heavy distortion of the lens and the need of a 1:1 scaling of the displayed image so that the projected HUD elements overlay those of the outside world. This presents a nonlinear problem accentuating the difficulty in determination of relevant HUD symbol positions on the image plane.

The chosen platform for flight data gathering was the R26S-Góbé type two-seater sailplane (glider). The visual images have been supplied by a wide angle lens camera externally mounted on the vertical stabilizer of the aircraft, facing in the direction of flight.

Regarding the terminology of the paper, the usual ECI, ECEF, NED and ABC (Aircraft Body or shortly Body) coordinate systems (frames) used for aerial navigation are used, see Figure 1. The frames are referred to by the indexes i, e, n, b .

Lacking an onboard navigation system, an external sensory system had been fitted on the aircraft in the form of an accelerometer, angular velocity meter, magnetometer (IMU) and differential GPS receivers. State estimation for the aircraft is based on a two level Extended Kalman Filtering with an additional external correction loop. The state estimator also supplies the data needed for displaying the Flight Path Vector in the form of flight path angle and drift information in degrees.

The problems to be solved are:

- accurately show the direction at which the nose of the aircraft is pointing (Boresighting);
- overlapping the vertical horizon line on the visible horizon line of the images supplied by the wide angle lens camera;
- displaying a set of compass values on the virtual horizon line so that the virtual cardinal directions shown overlap the actual cardinal directions seen from the aircraft;
- displaying the actual direction of flight by the means of a Flight Path Vector (FPV) by taking into account the drift and actual angle of attack of the aircraft.

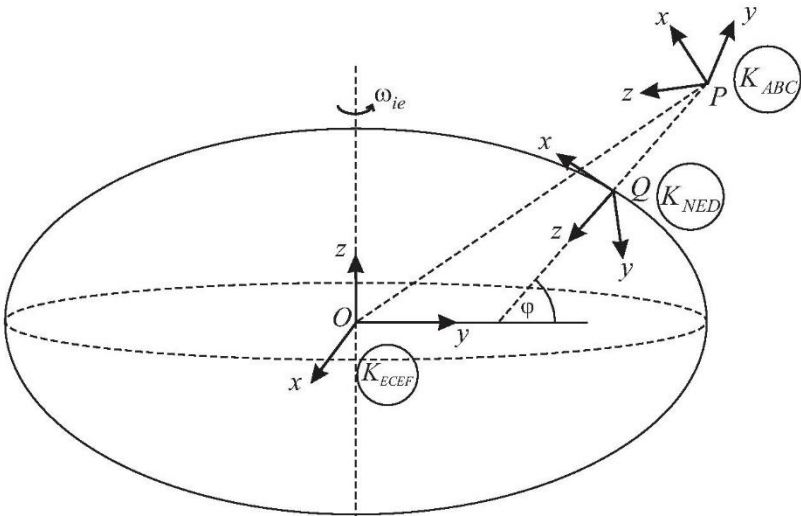


Figure 1. Coordinate systems used in navigation

The signals belonging to the body frame are shown in Figure 2, where Φ, Θ, Ψ denote the Euler (roll, pitch, yaw) angles, U, V, W represent the velocity, P, Q, R the angular velocity, X, Y, Z the force and L, M, N the torque components, v_T is the magnitude of the velocity, α is the angle of attack and β is the sideslip angle.

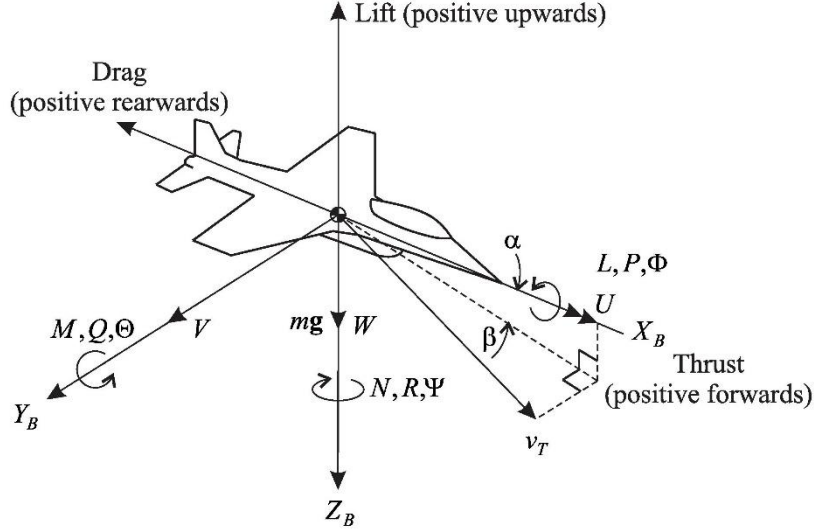


Figure 2. Aircraft frame and kinematic force/torque variables

DATA USED FOR DISPLAYING INFORMATION ON THE HEADS UP DISPLAY

For accurately displaying information needed to fly the airplane or unmanned aerial vehicle, the variables on the HUD use the data supplied by the state estimator. The supplied data consists of the following:

- measured GPS position in the K_e frame in $[m]$
- estimated velocity in the aircraft's K_b frame of reference along its three axis in m/s
- quaternion based orientation in K_b

The data supplied by the state estimator undergoes a transformation that allows it to be used on the HUD. Firstly, the position of the aircraft measured in the K_e frame has to be converted to the K_n frame used in aerial navigation. When displaying the height of the aircraft, the 'Down' axis position can be used. For using the QFE altimeter settings, the stationary position of the aircraft has been used as a reference point to zero the altimeter.

The velocity of the aircraft is displayed according to its x_b values and converted from m/s to km/h . Since the sensors available are not capable of measuring wind speed and direction, these values are also estimated and taken into account when displaying the velocity of the aircraft. Due to the fact the velocity of the aircraft is estimated in K_b and the wind speed in K_n , the following conversion needs to be implemented in order to get the correct data in K_b . By knowing the direction and intensity of the wind, the projections of the wind effect on the x_n, y_n axes are obtained:

$$v_{wind_n} = \begin{pmatrix} v_{wind} \cdot C_{wind_dir} \\ v_{wind} \cdot S_{wind_dir} \\ 0 \end{pmatrix} \quad (1)$$

Where the short forms C_{wind_dir} and S_{wind_dir} denote $\cos(x)$ and $\sin(x)$ respectively.

The aircraft velocity corrected for wind effects will be:

$$v_{a_w_n} = v_{a_n} + v_{wind_n} \quad (2)$$

Finally, the velocity of the aircraft corrected for wind effects in K_b will take the form of:

$$v_{aircr_b} = R_{b2n}^T \cdot v_{a_w_n} \quad (3)$$

where:

$$v_{aircr_b} = \begin{pmatrix} U_b \\ V_b \\ W_b \end{pmatrix} \quad (4)$$

and:

- v_{wind} – wind direction and intensity in K_n
- $v_{a_w_n}$ – aircraft velocity corrected for wind effects
- v_{a_n} – estimated aircraft velocity
- v_{wind_n} – estimated wind speed
- R_{b2n}^T – transpose of K_b to K_n transformation matrix

The vertical velocity indicator of the HUD uses the aircrafts velocity along its ‘Down’ axis in m/s after a conversion to the K_n frame.

The quaternion based orientation of the aircraft is firstly converted to Euler’s RPY angles in degrees and converted from K_b to the K_n frame using (5). This information is used to display heading and the virtual horizon elements of the HUD. In this article the notation for the RPY Euler angles will use Φ , Θ and Ψ .

$$\hat{q}_b \xrightarrow{R_{B2N}} \Phi_n, \Theta_n, \Psi_n \quad (5)$$

The β slip angle and α angle of attack is calculated according to the following [3]:

$$\alpha = atan\left(\frac{W_b}{U_b}\right) \quad (6)$$

$$\beta = asin\left(\frac{V_b}{v_{abs}}\right) \quad (7)$$

where:

$$v_{abs} = \|v_{aircr_b}\| \quad (8)$$

VIDEO CAMERA CALIBRATION AND BORESIGHTING

To be able to display the required data accurately, the internal and external parameters of the video camera have to be known. The internal parameters of the camera are: image size, focal length, principal point, skew, radial and tangential distortion coefficients. The video camera’s internal parameters are a priori identified using a chess board like picture rendition and the camera’s K matrix is regarded as known [5]:

$$K = \begin{bmatrix} f_x & \alpha_c \cdot f_x & c_x \\ 0 & f_y & c_y \\ 0 & 0 & 1 \end{bmatrix} \quad (9)$$

where:

f_x, f_y - identified focal length in pixels

c_x, c_y - principal point of the camera

α_c - skew

Viewing the complete distortion model of the lens it can be seen that a relevant radial distortion of up to 250 pixels is present in certain areas.

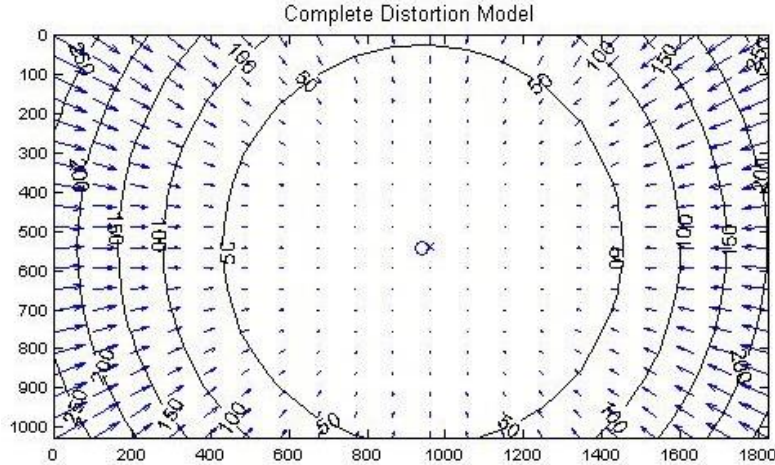


Figure 3. Identified complete distortion model of the wide angle lens camera

In order to obtain accurately aligned HUD elements, the aircraft, its sensors and the camera system need to be aligned with the aircraft's three axes – a process referred to as boresighting – so that the displayed data conforms to the reality of the captured image of the video camera. This allows the display to show the pilot exactly where the horizon is, the position of the cardinal directions as well as the aircraft's projected path with great accuracy.

The location of the IMU relative to the video camera is also known and taken into account and has its axes are aligned with the axes of symmetry of the aircraft.

Since the video camera had been mounted on the vertical stabilizer of the aircraft, a number of reference points can be singled out which are fixed to the aircraft's body coordinate system and are visible by the video camera. These reference points are required to be non-coplanar. The world coordinates of the 15 reference points are calculated based on the airplane design and are considered having the location of the video camera as the point of origin. The reference points can also be located on the captured images of the video camera (see Figure 4) so their pixel-coordinates can be measured. By knowing both the reciprocal world- and pixel coordinates of these reference points and the internal parameters of the wide angle lens video camera, the orientation of the video camera relative to the airplane can be determined. This process takes into consideration the internal camera parameters and uses the Least Squares method forming an abstract optimization problem. This can be solved with the Lagrange multiplier method and yields an optimal result with the use of singular value decomposition. The method is described in more detail in [1] and [7]. With the resulting R_{opt} rotation matrix the Φ and Ψ angular offsets of the HUD can be corrected.



Figure 4. Visual reference points used for Head Up Display boresighting

The arrangement of the video camera, the inertial measurement units and spatial arrangement of the visual reference points used for boresighting the Heads Up Display elements can be seen in Figure 5 as a 3D rendering of the mentioned points (the view of the 3D plot is from behind the airplane).

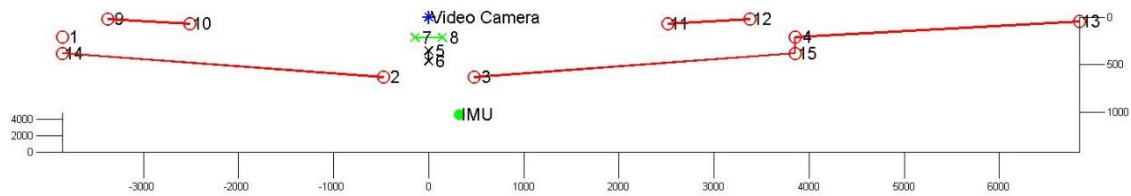


Figure 5. 3D rendering of reference points used for Head Up Display boresighting [mm]

PROJECTING THE VIRTUAL HORIZON LINE ON THE IMAGE PLANE CONSIDERING THE DISTORTION OF THE WIDE ANGLE LENS

While the display of altitude, airspeed, vertical velocity and heading on the HUD are mostly straightforward, the display of the artificial horizon also has to take into account the internal parameters of the wide angle lens camera. In order to have a useable system, the position and orientation of the artificial horizon line displayed on the image plane of the HUD has to be superimposed on the actual horizon line visible on the camera recording. The rendering of the virtual horizon line's vertical position uses the θ angle for pitch, while its slope is based on the ϕ bank angle, both derived from quaternions and converted in the NED frame.

The problem lies in the nonlinear distortion originating from the construction of the lens. As it can be seen in Figure 3, the distortion of the lens is mainly radial. For example, in level flight when $\theta = 0$ and $\phi = 0$, with a camera having its axes aligned with the axes of symmetry of the aircraft, we would have the rendering of the virtual horizon line in the center of the image plane superimposing the horizon line visible by the camera. But as the pitch of the aircraft is changed, a linear change in the vertical position of the virtual horizon line will present a nonlinearly increasing error in the difference between the positions of the actual and virtual horizon lines due to the radial distortion of the camera. Similarly, the spacing of the attitude indicator (or 'ladder') elements has to follow the nonlinearity of the distorted image even though they represent linear 10° increments of pitch. The cardinal directions on the virtual horizon line have to be placed in a way that they overlap the actual cardinal directions seen

from the aircraft and displaying the position the Flight Path Vector symbol showing the actual direction that the aircraft is going. In short, a solution needs to be found that converts the θ and ϕ angles supplied by the state estimator to the correct u, v pixel values while reducing the actual camera model to a pinhole camera. The transformation is illustrated in Figure 5.

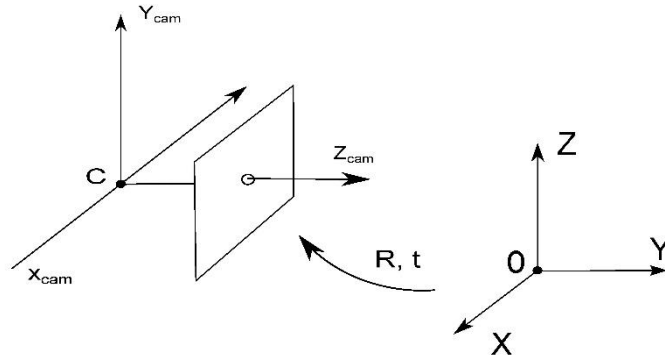


Figure 5. Transformation between world and camera coordinate frames

According to [2], the direct method for a Euclidian transformation between world and camera coordinate frames is used which also takes into account the mentioned lens distortion. The position and orientation of the camera is also considered:

$$\begin{bmatrix} X \\ Y \\ Z \end{bmatrix} = R \cdot \begin{bmatrix} X \\ Y \\ Z \end{bmatrix} + \begin{bmatrix} t_x \\ t_y \\ t_z \end{bmatrix} \quad (10)$$

Where:

R - represents the camera orientation matrix acquired using the boresighting process
 $(X, Y, Z)^T$ - world coordinates of the point P to be transformed to u, v pixel coordinates

$(t_x, t_y, t_z)^T$ - translation matrix of the camera

The mapping of the $(X, Y, Z)^T$ point from world coordinates to image plane is done by:

$$\begin{aligned} x' &= \frac{x}{z} \\ y' &= \frac{y}{z} \end{aligned} \quad (11)$$

Using the notations:

$$\begin{aligned} x'' &= x'(1 + k_1 r^2 + k_2 r^4) \\ y'' &= y'(1 + k_1 r^2 + k_2 r^4) \end{aligned} \quad (12)$$

where:

$$r^2 = x'^2 + y'^2 \quad (13)$$

The transformed u, v pixel coordinates will be:

$$\begin{aligned} u &= f_x \cdot x'' + c_x \\ v &= f_y \cdot y'' + c_y \end{aligned} \quad (14)$$

By definition, the horizon line is the line that separates earth from sky and has a critical importance in aviation in that it gives pilots a visual reference when keeping the wings of the aircraft leveled in horizontal flight or gives a visual indication of bank angle and pitch of the aircraft. Even though the actual horizon line is perceived as curved at higher altitudes and its curvature is accentuated due to the distortion effect of the wide angle lens, the virtual horizon line projected on the HUD needs to be a straight line. As a straight line, its position on the HUD image plane can be described using the vertical position of a single point P_H transformed to u, v image coordinates, in combination with the slope of a line intersecting P_H . In this paper, the

vertical position of P_H is in direct correlation with the θ pitch angle, while the slope is being determined by the Φ bank angle.

As it can be seen in Figure 6, an optimal alignment of the camera has its X_C, Y_C, Z_C axes running parallel to the Y_b, Z_b, X_b axes of the aircraft body. Any possible misalignments between the mentioned axes are detected by the boresighting method presented in the previous section. As mentioned before, the actual horizon line perceived by the wide angle lens camera is a straight line only when it is parallel with the X_C axis and runs through the principal axis of the camera. In any other case, the horizon line is perceived as either a convex or a concave curve depending on whether it is above or below the Z_C principal axis. This way, the rendition of the virtual horizon line on the HUD image plane is taking P_H as the point of tangency of a straight line to the actual horizon line with P_{H0} set on the principal axis of the camera when $\theta = 0$.

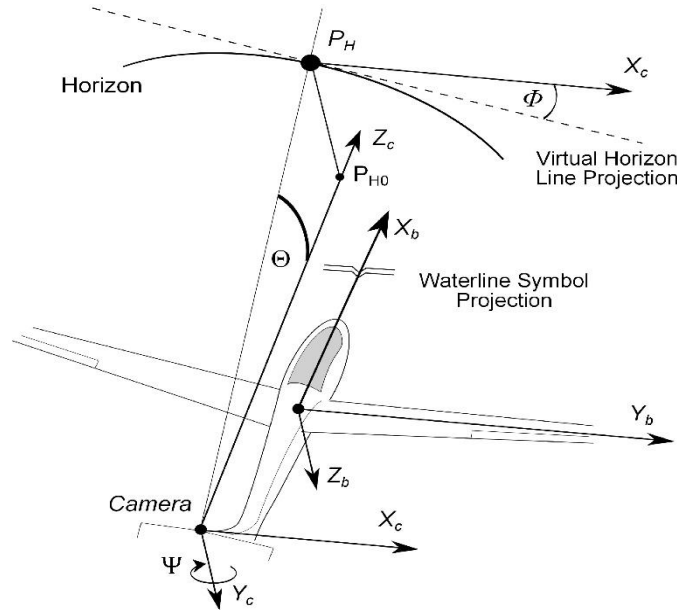


Figure 6. Video camera setup and Virtual Horizon Line projection concept

EXPERIMENTAL SETUP FOR VIRTUAL HORIZON LINE REPROJECTION ON IMAGES TAKEN WITH THE WIDE ANGLE LENS CAMERA

Once the transformation method from 3D world coordinates to u, v pixel coordinates is established, an experimental setup has been elaborated that reproduces the visual effect of the horizon as perceived by the airplane mounted camera. The concept for the experimental setup is based on the image of the actual horizon line as perceived by the camera. By studying the captured frames it is evident that the by changing the θ pitch angle of the aircraft, the horizon line performs a translational movement across the image plane as shown in Figure 7.



Figure 7. Movement of the horizon on the image plane as perceived by the wide angle lens video camera

This simplification is performed with regards to the fact that for pitch control the position of a single point P_H relative to the X_C axis of the camera is sufficient, noting that P_H is formed by the intersection between the visible horizon line and the Y_C, Z_C plane (see Figure 6). Due to the fact that P_H is a point, no perspective issues arise.

This has been modeled using the wide angle lens camera facing a chessboard like picture rendition, where the distance from camera to chessboard and the dimensions of chessboard squares are known. The modeling concept shown on Figure 8 has Z_1 as the distance from camera center to chessboard, and Y_1 and X_1 (not shown) are the distances from P_0 to P_1 in world coordinates. Point P_0 is set on the principal axis of the camera, having $X_1 = 0, Y_1 = 0$ and $t_{Y_1} = 0, t_{X_1} = 0$ where the $X_1, Y_1, Z_1, t_{X_1}, t_{Y_1}, t_{Z_1}$ values are the ones used in (9) with the boresight correction angles contained in the R matrix.

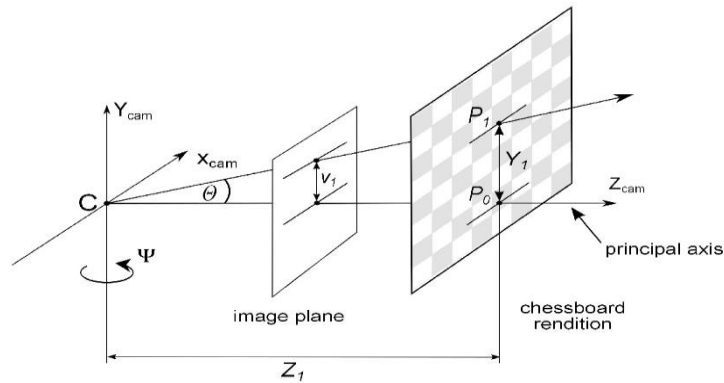


Figure 8. Re-projection of point P_1 on the image plane using a chessboard image

By using the proposed transformation method from world to pixel coordinates with the experimental setup and knowing the world coordinates of P_1 , its undistorted u, v coordinates can be obtained with θ derived from the C, P_0, P_1 triangle. Conversely, considering the C, P_0, P_1 triangle if the θ angle and the X_1, Z_1 , world coordinates of P_1 are known, then the vertical position of point P_1 , described by Y_1 can be calculated, reprojecting the point on the image plane, superimposing P_1 . Since the tangent function is not linear, its linearization is needed in order to precisely follow the chessboard pattern.

The reprojection method has been verified by re-generating the chessboard tile corners on the image taken with the wide angle lens camera. The results when the chessboard tiles are aligned with the X_{cam}, Y_{cam} axes of the camera are shown in Figure 9. Even in the areas of heavy distortion, the markers are superimposed on the intersections of chessboard tiles. The magenta + marker in the middle of the image is set on the principal point, while the green x marker is the first visual marker to be superimposed on the image. Its position is moved to the nearest intersection and all subsequent markers are generated using the iteration of linearized θ, ψ angles. The positioning of the starting marker to the intersection nearest the principal point is performed by the fine tuning of t_{X_1}, t_{Y_1} values.

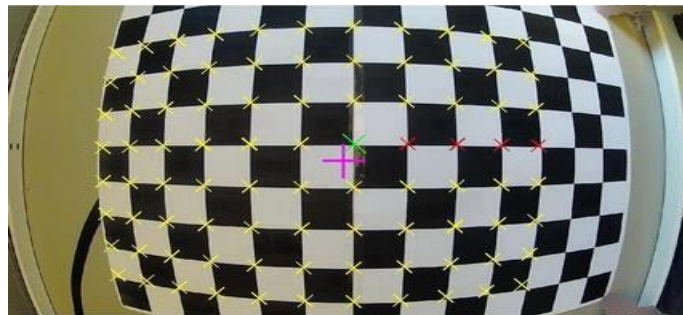


Figure 9. Reprojected world coordinate points on the image plane

In the event the aircraft presents a certain Φ roll angle, the slope of the virtual horizon line is performed by changing the roll angle in the camera orientation matrix R to the value of Φ . This is followed by the rendition of the virtual horizon line according to the pitch angle of the aircraft as described previously. The laboratory results can be verified using Figure 10, where the projected visual markers overlap the intersections of the chessboard tiles with the chessboard having a 69 deg. roll angle around the Z_{cam} camera axis.

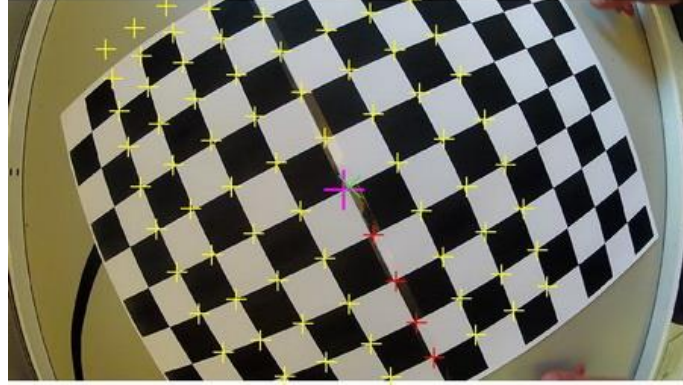


Figure 10. Reprojected world coordinate points on chessboard image with $\Phi = 69^\circ$

The transition from laboratory setup to real world application is based on the hypothesis that in the real world, the actual horizon line is always at a fixed distance from the aircraft: at a constant altitude, objects beyond the horizon line come into view at the traveling speed of the aircraft.

This way considering the C, P_{H0}, P_H , and C, P_0, P_1 seen in Figure 11, it can be concluded that the two are similar right angle triangles sharing the θ acute angle. Here, C represents the camera center, P_0, P_1 are seen as the world coordinate points found on the chessboard rendition with $(C, \widehat{P_0, P_1}) = 90^\circ$. Similarly P_{H0} represents a point on the horizon line when $\theta = 0$ and P_H is the same point on the horizon line when the attitude of the aircraft changes to a nonzero θ . In this concept $(C, \widehat{P_{H0}, P_H})$ is considered as a right angle.

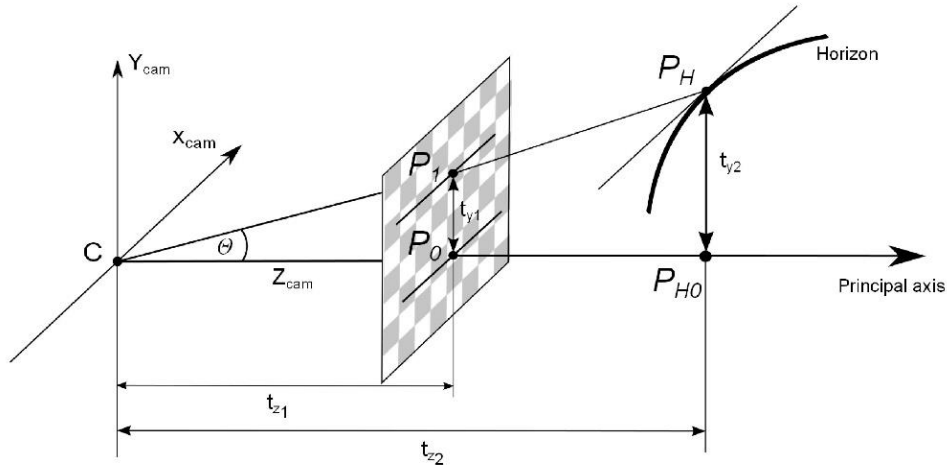


Figure 11. Linking the laboratory setup with the real world application

By viewing the horizon line reprojection problem as a similar right angle triangle problem, at any given θ , the required t_{z2}, t_{y2} distance variables to be used for the transformation of point P_H from world to image coordinates can be substituted with the pre-calibrated t_{z1}, t_{y1} distances of the laboratory setup.

HEADS UP DISPLAY APPLICATION USING ACTUAL FLIGHT DATA

Besides laboratory testing, the presented method has been verified by constructing a working Heads Up Display using the aircraft mounted wide angle lens video camera during flight and actual flight data.

The HUD elements superimposed on the images taken with the wide angle lens video camera can be seen in Figure 12 having the encircled numbers in the figure replaced by brackets in the text. As described in the introduction, the main HUD element responsible for helping the pilot maintain the orientation of the aircraft is the virtual horizon line {2} with the attitude indicator or ‘ladder’ {3}. These are used in conjunction with the waterline symbol to maintain the desired attitude of the aircraft. The application uses the position and inclination of the virtual horizon line as determined using the presented algorithm. Similarly, the spacing between ‘ladder’ elements is calculated the same way using 10 degree θ angle increments above and below the virtual horizon line. The waterline symbol {1} represents a small aircraft symbol positioned on the image plane in a way that its center is projected on the X_b axis of the aircraft and has its ‘wings’ parallel to Y_b (see Figure 6.). The position of this symbol on the image plane is determined in the boresighting phase.

When instrumental flight rules apply, in order to maintain a level flight all the pilot has to do is to align the ‘wings’ of the waterline symbol with the virtual horizon line. In level flight, the bank angle can be determined visually by the angle between the wings of the waterline symbol and virtual horizon line. Similarly, a desired pitch angle can be achieved by the pilot by aligning the waterline symbol with the ‘ladder’ element corresponding to the desired θ . Due to the fact that the ladder elements are always parallel with the virtual horizon line, in case the horizon is not in view of the camera and the virtual horizon line cannot be projected on the image plane, the ladder elements are to be used as secondary virtual horizon lines for control of the aircraft. The use of the aircraft attitude indicator and waterline symbol is presented in Figure 12, where the aircraft has a 13.5 degree pitch angle and a bank angle of 38 degrees.

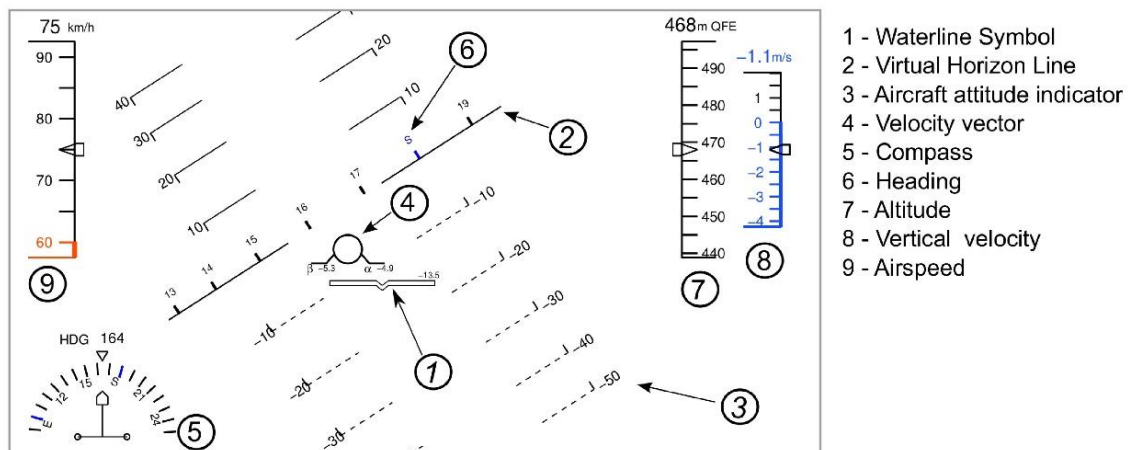


Figure 12. Projected Heads Up Display elements using actual flight data

As for the heading of the aircraft, the pilot can take visual cues from two HUD elements, a compass with a moving bezel {5} or from the heading values projected above the virtual horizon line {6} the position of which overlap the reference points of actual cardinal directions that are visible from the aircraft. The positioning of the cardinal values on the image plane is achieved using the presented method with a horizontal spacing of 10 degrees between compass points on the image. By placing the waterline symbol on a heading value projected on the virtual horizon line, the desired heading can be achieved.

The airspeed {9}, altitude {7} and vertical velocity {8} indicators have moving bezels with the actual values displayed numerically above the indicator boxes. All three indicators have scales moving behind a fixed arrow found in the middle of the indicator boxes. Moving scales have an advantage over numerical displays in being able to conveniently display the operating ranges of the aircraft, for example, by using a color coding on the airspeed indicator.

In this case, the 60 km/h stall speed of the aircraft is visible in orange and helps the pilot to intuitively determine how close the aircraft is to a stall. Minimum and maximum flaps and landing gear retraction and extension speeds can also be displayed using this method.

The Flight Path Vector or FPV {4} shows the aircraft as seen from behind and represents the direction the aircraft is actually moving as this does not always coincide with the direction the nose of the aircraft is pointing (Waterline symbol). Its use significantly reduces pilot workload on landing approaches and when flying in crosswinds. The position of the FPV coincides with that of the waterline symbol in cases when the angle of attack $\alpha = 0$ and the slip angle $\beta = 0$. The position of the FPV on the image plane and its deviation from its neutral position is also determined with the presented method according to the angular values of α and β .

Placement of the FPV along the pitch axis indicates the Flight path angle (FPA). When the FPV is on the horizon line, the FPA is zero (level flight). If the FPV is above the horizon line, the airplane is climbing; below the line, the airplane is descending regardless where the nose of the aircraft is pointing. The angle of climb or descent corresponds to where the center of the FPV intersects the pitch scale so flying the FPV to 3° below the horizon always produces a 3° glidepath. In the case presented in Figure 12, as a left hand turn is performed, even though its nose is pointing to -13.5 degrees, the flight path angle of the aircraft is only -4.5 degrees.

In the case presented in Figure 12, the FPV also shows that the aircraft is slipping, meaning that it is sideways to the relative airflow. This undesirable state can thus be visualized and corrected using the FPV.

RESULTS

By using the proposed method with a wide angle lens video camera mounted on a glider airplane during flight, together with gathered flight data, a useable Head Up Display has been realized containing all basic instrumentation required to operate a simple aircraft. The presented projection of HUD elements on the image plane had been applied to each frame captured by the video camera during flight, which resulted in a video recording. A frame from the video recording, showing the HUD elements seen in Figure 12 is presented on Figure 13.



Figure 13. Screenshot of HUD projected on the wide angle lens camera recording

The validation of the proposed method had been performed in two ways. Firstly, by visual verification of the alignment of the actual horizon with the position of the virtual horizon line, and secondly, by means of image processing.

The image processing algorithm firstly determines the pixel position of the horizon line on the image plane. Since, at times this line appears curved due to the distortion effect of the wide angle lens camera, a least squares approximation of multiple points found on the horizon is used to determine the position of point P_H . Point P_H is the point on the horizon set on the $X_b Y_b$ plane, as seen in Figure 6. By using the inverse of the proposed method, angle θ can be obtained while Φ can be calculated using the slope of the line determined with the least squares approximation. The image processing algorithm is performed on every frame of the video recording and the obtained Φ, θ angles are converted to K_n using equation (5). A screenshot of the image processing video can be seen in Figure 14, with the green dot representing point P_H , while the yellow line is the least squares approximation of the horizon line.

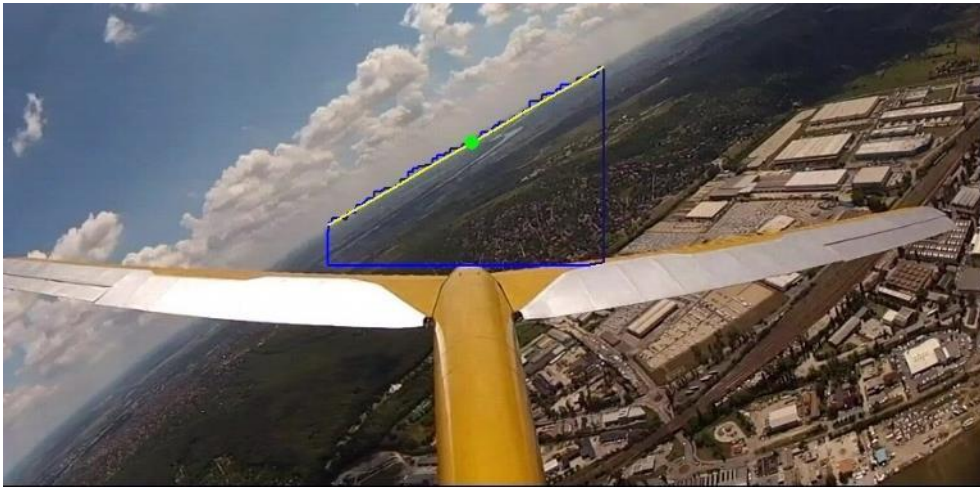


Figure 14. Image processing for horizon position and bank angle determination

Since the horizon line is not always visible due to the obstruction from view of the aircraft wings, data in these few cases is disregarded in later analysis.

Using the Φ, θ angle data obtained from image processing and from estimated flight data, the correlation of the two respective data sets has been determined to be 0.901 for the θ angle and 0.926 for Φ as shown in figures 15 and 16. However, since the flight data is obtained by a state estimator, the quality of obtained data is largely determined by the fine tuning of the multiple extended and classical Kalman filters. By improving the quality of estimated data, the correlation between the two data sets can be further improved.

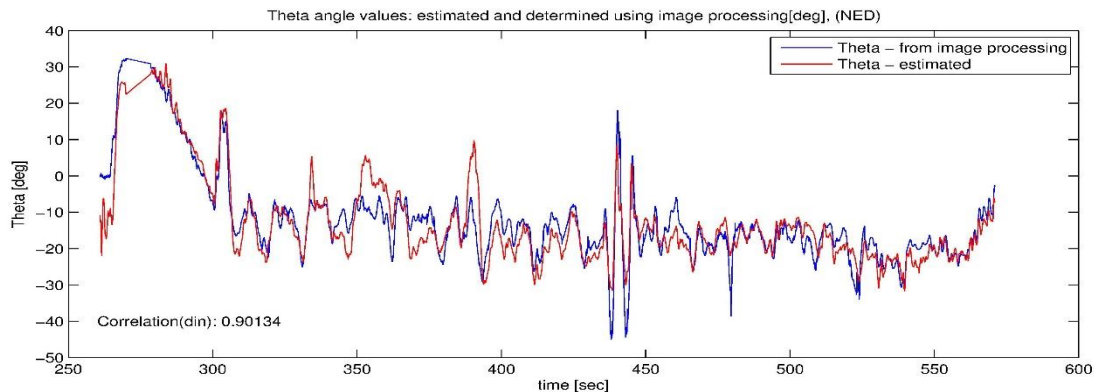


Figure 15. Correlation of θ angles, estimated vs. determined by image processing

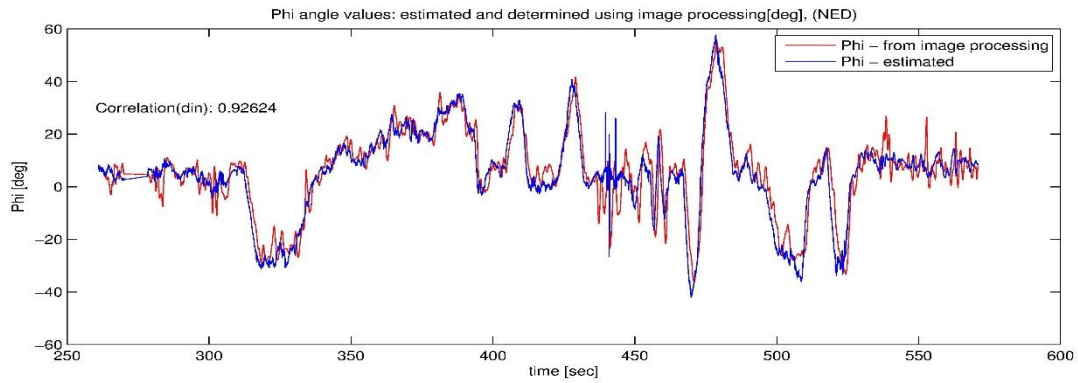


Figure 16. Correlation of Φ angles, estimated vs. determined by image processing

CONCLUSION

The paper presented methods and algorithms to solve the problem of a Heads Up Display projection on images taken with a wide angle lens camera. The method can prove especially useful in unmanned aerial vehicle control, where the use of a wide angle lens increases the field of view of the pilot thus increasing situational awareness. However, the use of a wide angle lens camera introduces severe distortion effects, a nonlinear problem that needs to be solved when placing the HUD elements responsible for attitude control on the image plane.

The paper gives a viable method for overcoming this problem, while realizing the 1:1 scaling of the displayed images so that the projected HUD elements overlay those of the outside world.

This is achieved at a low computational cost implementable on portable systems.

References

- [1] Tél F, *Stereo Image Processing System for Robotic Applications*, PhD Thesis. Budapest University of Technology and Economics, Department of Control Engineering and Information Technology, Budapest, 2009
- [2] R. Hartley and A. Zissermann, *Multiple View Geometry in Computer Vision*. Cambridge University Press, 2003
- [3] B. Lantos and L. Márton, *Nonlinear Control Of Vehicles and Robots*. London: Springer, 2011
- [4] Zhengyou Zhang, *On the Epipolar Geometry Between Two Images With Lens distortion*, Proc. Int'l Conf. Pattern Recognition (ICPR), Vol. I, pages 407-411, Aug. 1996, Vienna
- [5] Zhengyou Zhang, *A Flexible New Technique for Camera Calibration*, IEEE Transactions on Pattern Analysis and Machine Intelligence, Vol. 22, No. 11, November 2000
- [6] Heikkila, J. and Silven, O, *A four-step camera calibration procedure with implicit image correction*. CVPR97, 1997
- [7] L. Lukács and B. Lantos, *Data Fusion and Primary Image Processing for Aircraft Identification*. Periodica Polytechnica, electrical Engineering and Computer Science, 56/3, pages 83-94, Budapest 2012
- [8] Ed. Cary R. Spitzer, *The Avionics Handbook*. Boca Raton, CRC Press LLC. 2001

- [9] L. Lukács, State Estimation Method For Aircraft Identification Purposes. 9-th IEEE Symposium on Applied Computational Intelligence and Informatics, pages 31-35, May 15-17, Timisoara 2014
- [10] L. Lukács and B. Lantos, *Identification of the nonlinear dynamic model of sailplanes involving state estimation and image processing for actuator signal computation*. 12-th IEEE International Symposium on Intelligent Systems and Informatics, accepted for publication, September 11-13, Subotica 2014